iScience

CellPress
OPEN ACCESS

Article

IP_3R-mediated Ca^{2+} signaling controls B cell proliferation through metabolic reprogramming

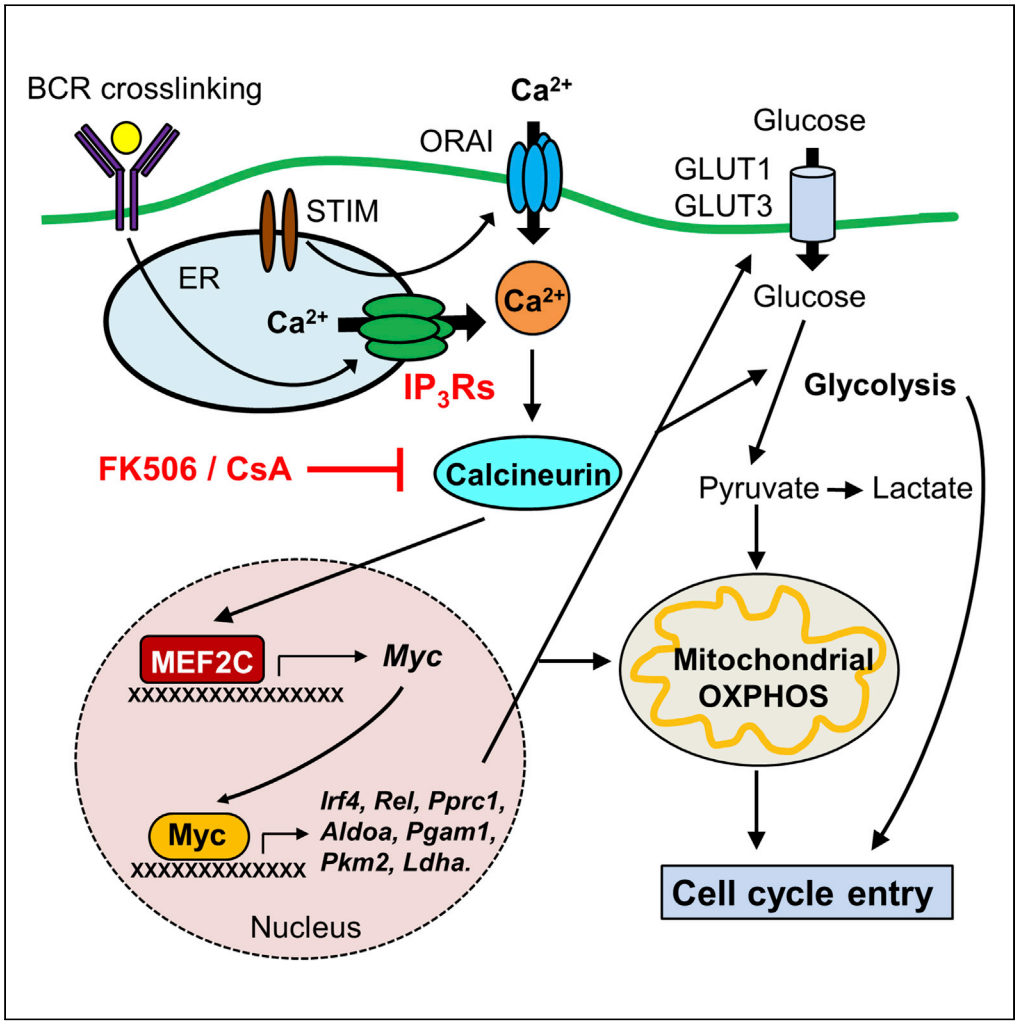

Huayuan Tang, Yali Li, Shijia Wang, ..., Xi Fang, Lu Sun, Kunfu Ouyang

tanghuayuan33@126.com (H.T.)
sunlu19802003@163.com (L.S.)
ouyang_kunfu@pku.edu.cn (K.O.)

Highlights

IP_3R-Ca^{2+} is pivotal for B cell activation by regulating metabolic reprogramming

IP_3R-Ca^{2+} governs glucose uptake, glycolytic gene expression, and mitochondrial remodeling

IP_3R-Ca^{2+} targets the calcineurin-MEF2C-Myc pathway in driving metabolic adaptations

Tang et al., iScience 25, 104209
May 20, 2022
https://doi.org/10.1016/j.isci.2022.104209

iScience

CellPress
OPEN ACCESS

Article

IP_3R-mediated Ca^{2+} signaling controls B cell proliferation through metabolic reprogramming

Huayuan Tang,[1,2,6,7,*] Yali Li,[1,2,6] Shijia Wang,[1,6] Jing Ji,[1] Xiangbin Zhu,[1] Yutong Bao,[3] Can Huang,[1] Ye Luo,[1] Lei Huang,[1] Yan Gao,[5] Chaoliang Wei,[4] Jie Liu,[4] Xi Fang,[3] Lu Sun,[1,*] and Kunfu Ouyang[1,*]

SUMMARY

Emerging evidence shows that metabolic regulation may be a critical mechanism in B cell activation and function. As targets of several most widely used immunosuppressants, Ca^{2+} signaling and calcineurin may play an important role in regulating B cell metabolism. Here, we demonstrate that IP_3R-mediated Ca^{2+} signaling and calcineurin regulate B cell proliferation and survival by activating metabolic reprogramming in response to B cell receptor (BCR) stimulation. Both IP_3R-triple-knockout (IP_3R-TKO) and calcineurin inhibition dramatically suppress the metabolic switch in oxidative phosphorylation and glycolysis of stimulated B cells through regulation of glucose uptake, glycolytic enzyme expression, and mitochondrial remodeling, leading to impaired cell-cycle entry and survival. In addition, IP_3R-Ca^{2+} acts as a master regulator of the calcineurin-MEF2C-Myc pathway in driving B cell metabolic adaptations. As genetic defects of IP_3Rs were recently identified as a new class of inborn errors of immunity, these results have important implications for understanding the pathogenesis of such diseases.

INTRODUCTION

Appropriate activation of B cells is important for maintaining immune homeostasis free from immunodeficiency and autoimmune diseases (Baba and Kurosaki, 2016; LeBien and Tedder, 2008). Recent studies have shown that metabolic programming may be a critical mechanism involved in B cell activation and function (Caro-Maldonado et al., 2014; Dufort et al., 2014; Jellusova, 2020). In comparison with mature naive B cells, which remain in a quiescent state with low metabolic requirements, activated B cells upregulate both glycolysis and oxidative phosphorylation in a balanced fashion (Caro-Maldonado et al., 2014), whereas interfering with metabolic pathways via inhibiting glycolysis (Jayachandran et al., 2018) or mitochondrial respiration (Diaz-Munoz et al., 2015) has been shown to disturb B cell proliferation and immune responses, suggesting that metabolic programming may be important for B cell activation. In addition, metabolism is not only required for meeting energy demands but has also been integrated into the signaling cascades of many intracellular messengers including ATP, NADP + -NADPH, and reactive oxygen species (ROS), reflecting changes in extracellular environment or intracellular metabolic status and dictating cellular fate (Wang and Green, 2012).

One of the central downstream signaling events in response to BCR ligation is intracellular Ca^{2+} elevation, which is generated by Ca^{2+} release from the ER Ca^{2+} store and a subsequent store-operated Ca^{2+} entry (SOCE) following the depletion of ER Ca^{2+} stores (Baba and Kurosaki, 2011). Inositol 1,4,5-trisphosphate receptors (IP_3Rs) are the main ER Ca^{2+} release channels with three subtypes in B cells, which we previously demonstrated are essential for BCR-mediated Ca^{2+} mobilization and B cell development (Tang et al., 2017). Loss of all three subtypes of IP_3Rs leads to completely abolished Ca^{2+} release from ER Ca^{2+} stores, as well as subsequent SOCE, and reduces recirculating mature B cell numbers and alters antibody production (Tang et al., 2017). Notably, heterozygous variants in IP_3R have recently been identified in patients with combined immunodeficiency (Neumann et al., 2021), where disrupted calcium homeostasis and abnormal proliferation and activation of B and T cells were observed. This finding demonstrates that human lymphocytes are indeed sensitive to defects in the primary ER Ca^{2+} release system; however, underlying mechanisms that are critical for treatment and intervention have not yet been clearly identified.

Increasing intracellular Ca^{2+} concentrations subsequently activate the serine-threonine phosphatase calcineurin, which participates in a number of Ca^{2+}-dependent signal transduction pathways, particularly in

[1]Department of Cardiovascular Surgery, Peking University Shenzhen Hospital, State Key Laboratory of Chemical Oncogenomics, School of Chemical Biology and Biotechnology, Peking University Shenzhen Graduate School, Shenzhen, China

[2]Institute of Neurological and Psychiatric Disorders, Shenzhen Bay Laboratory, Shenzhen 518132, China

[3]Department of Medicine, School of Medicine, University of California San Diego, La Jolla, CA, USA

[4]Department of Pathophysiology, School of Medicine, Shenzhen University, Shenzhen, China

[5]Department of Cardiovascular Medicine, Shenzhen Qianhai Shekou Free Trade Zone Hospital, Shenzhen Shekou People's Hospital, Shenzhen, China

[6]These authors contributed equally

[7]Lead contact

*Correspondence: tanghuayuan33@126.com (H.T.), sunlu19802003@163.com (L.S.), ouyang_kunfu@pku.edu.cn (K.O.)

https://doi.org/10.1016/j.isci.2022.104209

regulating the transcription factor NFAT during T cell activation (Vaeth and Feske, 2018). Notably, two of the most widely used immunosuppressive drugs, cyclosporine A (CsA) and FK506, target calcineurin and have been shown to selectively abrogate Ca^{2+}-regulated activation pathways in both B cells and T cells (Klaus et al., 1994), but we still lack a thorough and complete understanding of their mechanism of action. Whether this involves IP_3R-Ca^{2+} signals that modulate metabolic adaptations during B cell activation and proliferation is largely unexplored.

In the present study, we use B cell-specific IP_3R-TKO mice to show that IP_3R-mediated Ca^{2+} signaling and calcineurin are essential for B cell proliferation by triggering metabolic reprogramming in response to BCR stimulation. IP_3R-Ca^{2+} and calcineurin control B cell metabolic reprogramming through regulating glucose uptake, glycolytic enzyme expression, as well as mitochondrial remodeling, likely involving the regulation of c-Myc, which is dependent on the calcineurin-MEF2C pathway. We present a paradigm whereby loss of IP_3Rs and calcineurin inhibition leads to defective B cell proliferation and function upon antigen infection as a result of the inactivation of metabolic reprogramming, underpinning IP_3R-Ca^{2+} as an important metabolic trigger for B cell activation and proliferation, which may provide novel insights into the etiology of immune-related diseases.

RESULTS

Metabolic reprogramming activated by IP_3R-Ca^{2+}-calcineurin is required for BCR-induced cell cycle entry

To first investigate whether IP_3R-mediated Ca^{2+} signaling controls BCR-mediated proliferation via calcineurin, we measured calcineurin activity in IP_3R-TKO B cells and found it was significantly impaired compared to control (Figures S1A and S1B), confirming that calcineurin is indeed downstream of IP_3R-Ca^{2+}. To verify the role of IP_3R-Ca^{2+} signaling and calcineurin in controlling BCR-mediated proliferation, we performed a proliferation assay in control and IP_3R-TKO B cells with or without the treatment of calcineurin inhibitor, FK506. In accordance with our previous findings (Tang et al., 2017), BCR-mediated upregulation of the cell cycle marker Ki-67 was dramatically blocked in IP_3R-deficient B cells compared to control (Figures 1A and 1B). In addition, FK506 also completely blocked BCR-induced upregulation of Ki-67 in B cells (Figures 1A and 1B), demonstrating a defect in antigen-dependent cell-cycle entry in B cells upon the loss of IP_3R-mediated Ca^{2+} release or inhibition of calcineurin. Along with proliferation, we also found that cell survival was impaired in both IP_3R-deficient and FK506-treated B cells after BCR stimulation, as indicated by reduced percentages of live cells by the LIVE/DEAD staining (Figures S1C and S1D). In addition, deletion of all IP_3Rs or another calcineurin inhibitor CsA could significantly reduce the expression of antiapoptotic genes, *Bcl2la1* and *Bcl2l1* (Figure S1E), suggesting that IP_3R-Ca^{2+} release and calcineurin also play an important role in regulating B cell survival. We further investigated whether BCR expression was affected in the loss IP_3Rs. Interestingly, we found a significantly elevated rather than reduced IgM expression in IP_3R-TKO B cells compared to control (Figure S1F), suggesting that the defect in BCR-induced proliferation and survival in IP_3R-TKO B cells was not due to impaired BCR expression.

Cells have to pass a metabolic checkpoint and meet nutrient sufficiency before progressing through G1 and committing to mitosis (Foster et al., 2010). Glycolysis is the main source of anabolic metabolism after B cell activation, for which the primary source of energy and carbon is glucose (Jellusova, 2020). Consistently, 2-deoxy-D-glucose (2-DG), a glucose analog that suppresses glycolysis (Wick et al., 1957), could dramatically inhibit both cell cycle entry (Figures 1C and 1D) and survival (Figures S1G and S1H) of BCR-activated B cells, confirming that glucose uptake and utilization is required for cell-cycle commitment and survival of B cells. To test whether IP_3R and calcineurin contribute to this metabolic switch of B cells, we examined oxidative phosphorylation (OXPHOS) and aerobic glycolysis of B cells using the Seahorse Extracellular Flux analyzer. Mitochondrial oxygen consumption rate (OCR) and extracellular acidification rate (ECAR) were first measured in B cells following 6 h of BCR stimulation. At this time point, B cells have not entered the cell cycle, and therefore metabolic changes are not caused by potential secondary effects of proliferation (Caro-Maldonado et al., 2014). In comparison to unstimulated B cells, BCR stimulation indeed significantly increased both basal and maximal OCR (Figures 1E and 1F). However, BCR stimulation-induced increases in basal and maximal OCR were completely abolished in IP_3R-TKO B cells (Figures 1E and 1F). In addition, BCR stimulation induced a dramatic increase in basal ECAR of control B cells, which was also impaired in IP_3R-TKO B cells (Figures 1G and 1H). Combined analysis of the respiratory capacity and glycolytic function of stimulated B cells clearly separated control cells from IP_3R-TKO B cells, the latter of which resembled more closely to resting cells (Figure 1I). In addition, calcineurin inhibitor FK506 or CsA also

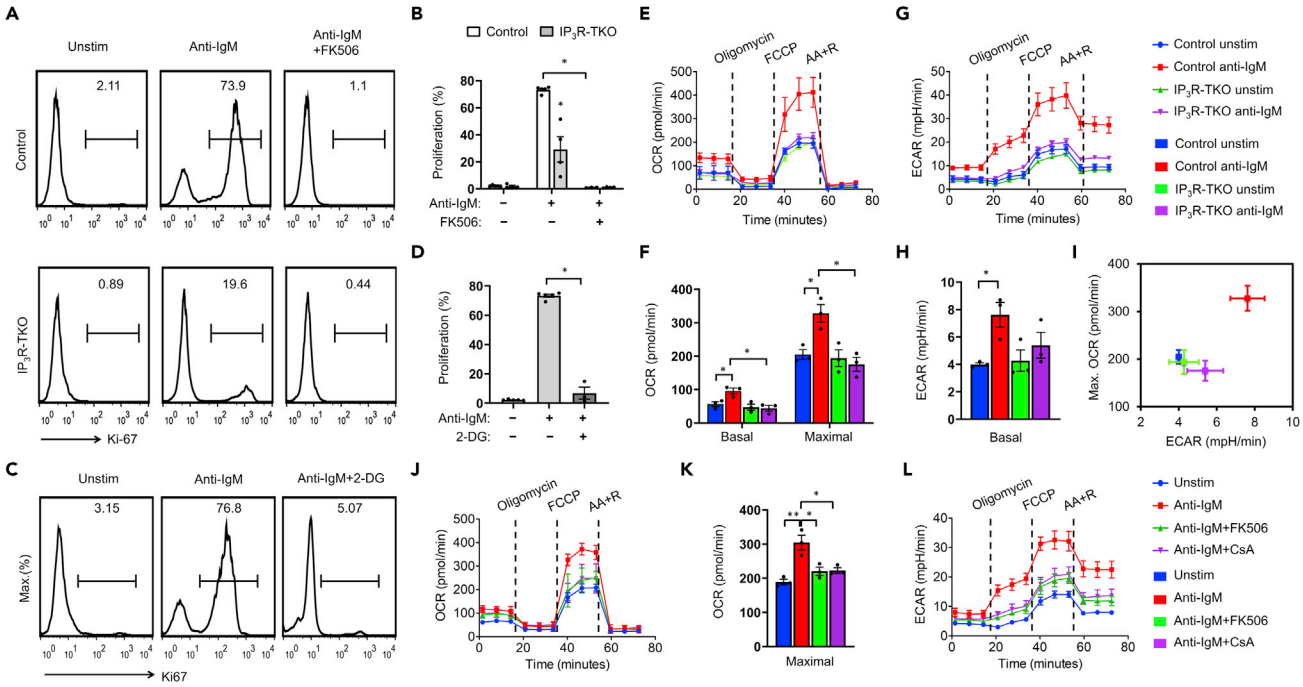

Figure 1. IP_3Rs and calcineurin control BCR-induced cell cycle entry through metabolic reprogramming

(A) Cell proliferation as assessed by Ki-67 expression. Splenic B cells from control and IP_3R-TKO mice were left unstimulated or were stimulated for 48 h with anti-IgM (20 μg/mL) in the presence or absence of FK506 (1.25 μM).

(B) Quantification of Ki-67^+ cells in (A). Mean ± SEM, n = three to five mice per group.

(C) Ki-67 expression in control splenic B cells left unstimulated or stimulated with anti-IgM (20 μg/mL) for 48 h in the presence or absence of 2-DG (10 mM).

(D) Quantification of Ki-67 + cells in (C). Mean ± SEM, n = three to five mice per group.

(E–H) Extracellular flux analysis of (E) oxygen consumption rate (OCR), (F) basal and maximal respiration, (G) extracellular acidification rate (ECAR), and (H) basal ECAR of control and IP_3R-TKO splenic B cells left unstimulated or stimulated with anti-IgM (20 μg/mL) for 6 h. Mean ± SEM, n = 3 mice per group.

(I) Maximal OCR plotted against ECAR from data in (G) and (H).

(J–L) Extracellular flux analysis of (J) oxygen consumption rate (OCR), (K) maximal respiration, and (L) extracellular acidification rate (ECAR) of control splenic B cells left unstimulated or stimulated with anti-IgM (20 μg/mL) for 6 h in the presence or absence of FK506 (1.25 μM) or CsA (1 μM).

Mean ± SEM, n = 3 mice per group. *$p < 0.05$, **$p < 0.01$.

exhibited a similar inhibitory effect on such activation-induced increases in OCR and ECAR in B cells (Figures 1J–1L). Taken together, these results clearly demonstrate that IP_3R-Ca^{2+} and calcineurin are required for the metabolic switch of B cells as a precondition for cell-cycle entry and survival.

IP_3Rs and calcineurin modulate glucose uptake and glycolytic enzyme expression

One essential pathway to increase glycolysis is through increased glucose uptake. Given that 2-DG could dramatically inhibit both cell cycle entry (Figures 1C and 1D) and cell survival in BCR-activated B cells (Figures S1G and S1H), we hypothesized that IP_3R and calcineurin might directly control glucose uptake in B cells. To test this, we first evaluated the ability of glucose uptake in B cells using the fluorescent glucose analogue 2-NBDG and found that BCR stimulation induced a ~3-fold increase of glucose uptake in control B cells, which was almost absent in IP_3R-TKO or CsA-treated B cells (Figure 2A), suggesting that IP_3R-Ca^{2+} release and calcineurin activation are essential for glucose uptake in activated B cells.

GLUT1 plays an important role in controlling glucose uptake in various types of cells including B cells, with induced expression upon BCR stimulation (Akkaya et al., 2018; Caro-Maldonado et al., 2014). Indeed, we also found that GLUT1 expression was significantly upregulated in BCR-stimulated control B cells when compared with unstimulated cells (Figure 2B). In addition, expression of GLUT3, another important player in regulating glucose uptake (Akkaya et al., 2018), was also significantly elevated in response to BCR stimulation (Figure 2C). Consistent with the defects of glucose uptake observed in IP_3R-TKO and CsA-treated B cells, upregulation of GLUT1 and GLUT3 expression upon BCR stimulation was also significantly reduced by IP_3R deletion and calcineurin inhibition (Figures 2B and 2C), which is in agreement with defects in

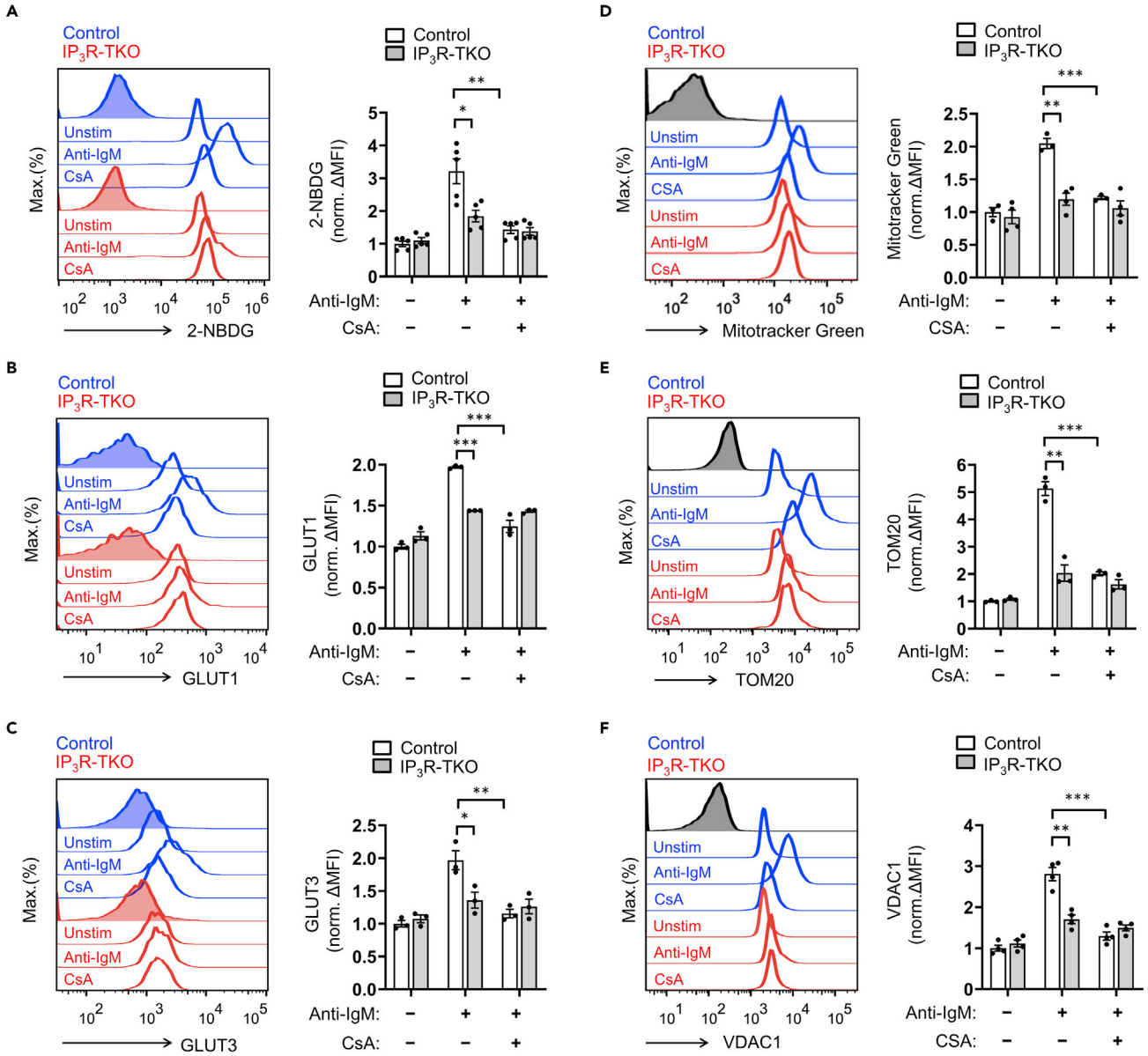

Figure 2. IP_3Rs and calcineurin facilitate glucose uptake and mitochondrial mass increase in activated B cells

(A–F) Splenic B cells from control and IP_3R-TKO mice were left unstimulated or were stimulated with anti-IgM (20 μg/mL) for 20 h in the presence or absence of CsA (1 μM), and analyzed by flow cytometry for (A) glucose uptake (as measured by 2-NBDG uptake), (B) GLUT1 protein expression, (C) GLUT3 protein expression, (D) mitochondrial volume using Mitotracker Green, expression of (E) TOM20, and (F) VDAC1. n = 5 mice per group of three repeat experiments in (A). n = 3 mice per group in (B and C). n = three to four mice per group in (D–F).

Mean ± SEM, *p < 0.05, **p < 0.01, ***p < 0.001.

glucose uptake and cell growth (Figures 2A and S2A). Because glycolysis is the major pathway for glucose metabolism in which glucose will convert to pyruvate (under aerobic condition) or lactate (anaerobic) through a series of enzyme-catalyzed reactions (Donnelly and Finlay, 2015), we investigated whether deletion of IP_3Rs and calcineurin inhibition could also affect the expression of the glycolytic enzymes. We found BCR stimulation significantly upregulated the expression of hexokinase (*Hk2*), aldolase A (*Aldoa*), phosphoglycerate mutase 1 (*Pgam1*), pyruvate kinase M2 (*Pkm2*), and lactate dehydrogenase A (*Ldha*) in control B cells (Figure S2B), whereas such increases were severely impaired in IP_3R-TKO or CsA-treated B cells (Figure S2B). Therefore, these results indicate that IP_3R and calcineurin modulate glucose uptake and regulate

the induction of gene expression of both glucose transporters and glycolytic enzymes in B cells upon BCR stimulation to control glucose uptake.

IP_3Rs and calcineurin are required for BCR-induced increases in mitochondrial mass and mitochondrial enzyme expression

B cell metabolic reprogramming is a balanced process involving increased expression of both glycolytic and mitochondrial components (Jellusova and Rickert, 2017). Given that B cell stimulation enhanced mitochondrial respiration, which was abolished in both IP_3R-deficient and CsA-treated B cells (Figures 1E and 1J), we next investigated the role of IP_3R-mediated Ca^{2+} signaling and calcineurin in mitochondrial metabolism of B cells. Because mitochondrial mass is correlated with cell metabolic activity (Caro-Maldonado et al., 2014), we quantified mitochondrial mass by Mitotracker Green staining. Consistent with previous reports (Akkaya et al., 2018; Caro-Maldonado et al., 2014), B cell activation led to a significant elevation in mitochondrial mass as evidenced by increased fluorescence with Mitotracker Green upon BCR stimulation in control B cells (Figure 2D). However, no such increase could be observed in IP_3R-TKO B cells or B cells treated with CsA (Figure 2D). In addition, the flow cytometry analysis of mitochondrial protein TOM20 and VDAC1 also showed the same trends among control, IP_3R-TKO, and CsA-treated B cells (Figures 2E and 2F), further confirming that IP_3R-mediated Ca^{2+} signaling and calcineurin are essential for BCR-induced increase in mitochondrial mass.

We then analyzed the expression of mitochondrial electron transport chain (ETC) complexes. Interestingly, BCR stimulation increased the protein levels of ATP5A (complex V) and UQCRC2 (complex III) in control B cells, whereas NDUFB8 (complexes I), SDHB (complex II), and MTCO1 (complex IV) remained unchanged (Figures S2C and S2D). Such increases in ATP5A and UQCRC2 expression upon BCR stimulation was also accompanied with upregulation of PPRC1 mRNA levels (Figures S2C–S2E), one of the PGC-1 family of transcriptional co-regulators that has been reported to regulate the expression of mitochondrial ETC complexes and mitochondrial biogenesis (Scarpulla, 2011). Notably, increased expression of ATP5A, UQCRC2, or PPRC1 was significantly impaired in IP_3R-TKO and CsA-treated B cells (Figures S2C–S2E), which was consistent with the changes in mitochondrial respiration and mitochondrial mass (Figures 1E, 1J, and 2D). Our results thus strongly suggest that IP_3R- Ca^{2+} and calcineurin control mitochondrial respiration by regulating mitochondrial mass and ETC complexes upon BCR stimulation. Importantly, ionomycin treatment of IP_3R-TKO B cells could efficiently restore the defects in BCR-induced cell growth, glucose uptake, and mitochondrial mass increase (Figures S3A–S3C), validating a central role for Ca^{2+} in B cell metabolic programming.

c-Myc is required for IP_3R and calcineurin-dependent metabolic reprogramming

To understand the molecular mechanism responsible for the defect of metabolic switch induced by IP_3R deletion, we analyzed the transcriptional regulation of several metabolic regulators, including c-Myc (Jellusova, 2020), Irf4 (Low et al., 2019), and c-Rel (Gu et al., 2021; Li et al., 2020). We first measured the mRNA expression of these metabolic regulators; although BCR stimulation increased the mRNA levels of all these genes in control B cells, these increases were significantly attenuated in IP_3R-TKO and CsA-treated B cells (Figures 3A and S4A). We then measured the c-Myc protein expression and found a similar result among control, IP_3R-TKO, and CsA-treated B cells (Figures 3B and 3C). c-Myc has been proposed to play an essential role in regulating the metabolic reprogramming following B cell activation (Caro-Maldonado et al., 2014). We therefore speculated that impaired c-Myc induction may be responsible for the defects of metabolic reprogramming observed in IP_3R-TKO or calcineurin-inhibited B cells. By using a small molecule c-Myc inhibitor 10,058-F4, we found that c-Myc inhibition was sufficient to block the increases in glucose uptake (Figure 3D), expression of GLUT1 and GLUT3 (Figures 3E and 3F), and expression of glycolytic enzymes induced by BCR stimulation in control B cells (Figure S4B). In addition, BCR stimulation-induced increases in cell growth (Figure S4C), mitochondrial mass (Figure 3G), and expression of mitochondrial proteins (Figures 3H and 3I) and *Pprc1* (Figure S4D) were all significantly inhibited by 10,058-F4 in control B cells. More importantly, we found that BCR-induced expression of *Irf4* and *Rel* was also dramatically impaired by 10,058-F4 (Figure S4E). Taken together, these results suggest that c-Myc could play a central role in controlling metabolic reprogramming in B cells upon BCR stimulation in an IP_3R and calcineurin-dependent manner.

IP_3R-dependent MEF2C expression modulates c-myc induction

Given the established involvement of the PI3K-AKT-mTOR signaling pathway in controlling metabolic reprogramming as well as c-Myc expression (Berry et al., 2020; Vaeth et al., 2017), we next investigated

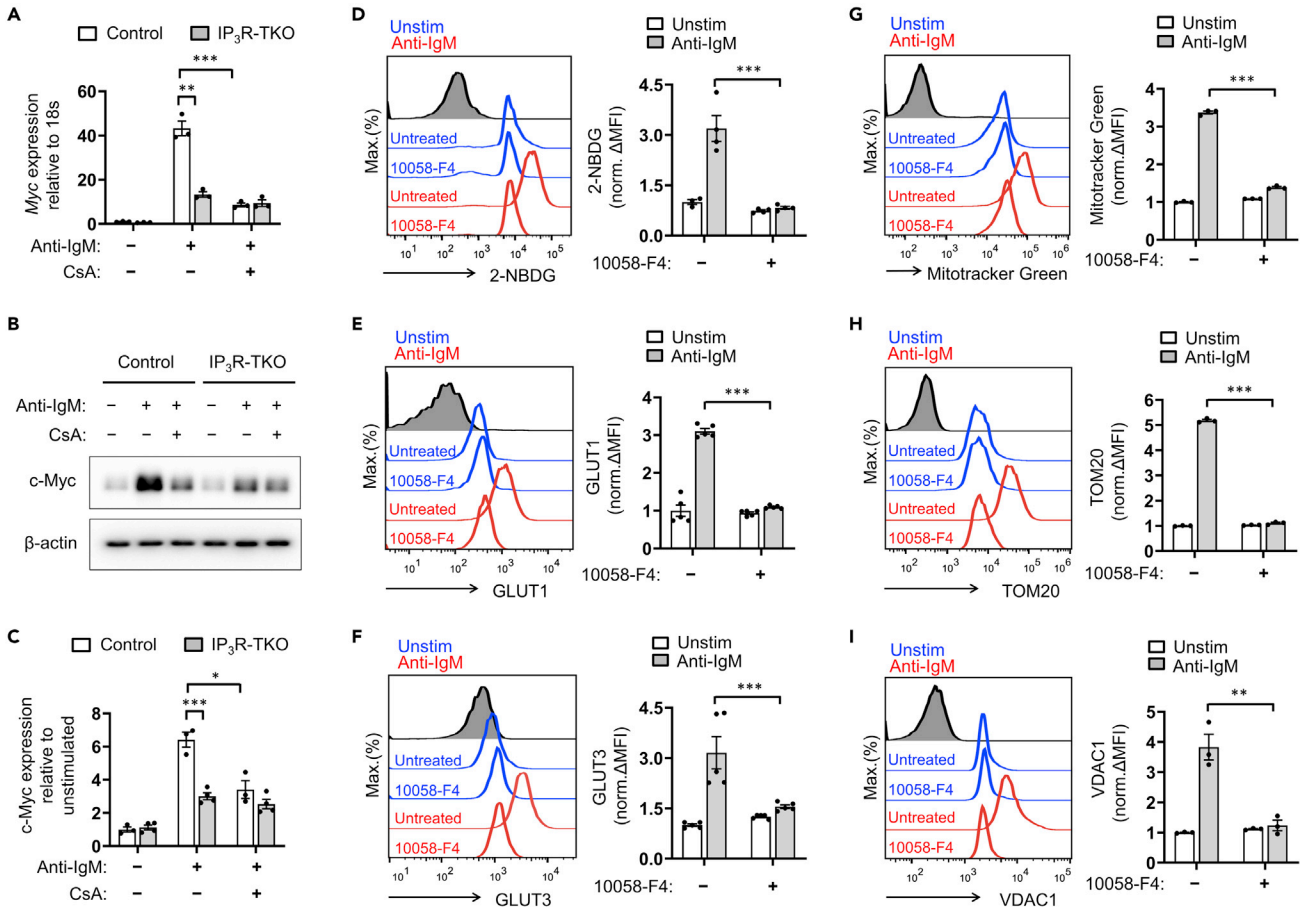

Figure 3. IP_3Rs and calcineurin control BCR-induced metabolic switch through c-Myc

(A) Splenic B cells from control and IP_3R-TKO mice were left unstimulated or were stimulated with anti-IgM (20 μg/mL) for 3 h in the presence or absence of CsA (1 μM) and analyzed by qRT-PCR for *Myc* expression. Mean ± SEM, n = 3 mice per group.

(B and C) Splenic B cells from control and IP_3R-TKO mice were left unstimulated or were stimulated with anti-IgM (20 μg/mL) for 2 h in the presence or absence of CsA (1 μM) and analyzed by western blot for expression of c-Myc. (B) Representative immunoblots. (C) Densitometric analyses. Mean ± SEM, n = 3 mice per group.

(D–I) Splenic B cells from control mice were left unstimulated or were stimulated with anti-IgM (20 μg/mL) for 24 h in the presence or absence of 10,058-F4 (100 μM), and were analyzed by flow cytometry for (D) glucose uptake, (E) GLUT1 protein expression, (F) GLUT3 protein expression, (G) mitochondrial volume, (H) TOM20, and (I) VDAC1 expression.

Mean ± SEM, n = three to five mice per group. For all figures, *p < 0.05, **p < 0.01, ***p < 0.001.

whether impaired induction of c-Myc expression was caused by inactivation of the PI3K-AKT-mTOR pathway because of the loss of IP_3Rs. Surprisingly, we observed an increased activation of the PI3K-AKT-mTOR pathway in IP_3R-TKO B cells after BCR stimulation as evidenced by elevated phosphorylation of AKT and the ribosomal S6 protein (Figure 4A), indicating that PI3K-AKT-mTOR pathway may not be directly involved in induction of c-Myc expression in stimulated B cells.

Calcineurin-regulated transcription factor MEF2C has been previously reported to regulate B cell proliferation and survival in response to BCR stimulation (Blaeser et al., 2000; Wilker et al., 2008), and enforced expression of MEF2C in transitional B cells leads to increased c-Myc expression after BCR cross-linking (Andrews et al., 2012). To investigate whether IP_3R and calcineurin may regulate c-Myc expression through MEF2C-dependent pathways, we first performed ChIP-qPCR analysis and found that that MEF2C binds to the promoter region of *Myc* gene (Figure 4B), suggesting a direct regulation of *Myc* expression by MEF2C. Intriguingly, MEF2C protein expression was significantly decreased in IP_3R-TKO B cells compared to control B cells (Figures 4C and 4D). Consistent with this, the amount of ChIPped *Myc* DNA by MEF2C was also significantly reduced in IP_3R-TKO B cells (Figure 4B). We then investigated whether reduced expression of MEF2C protein observed in

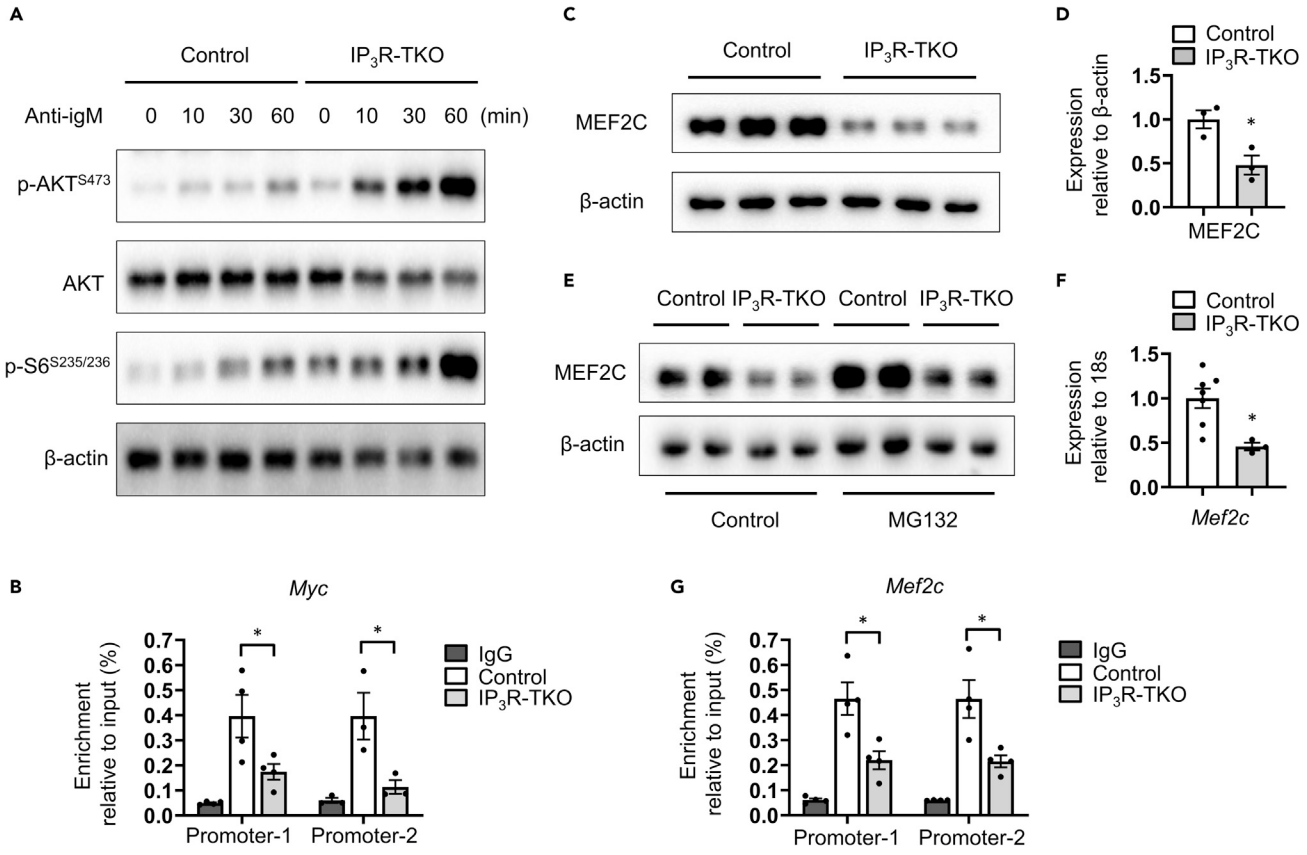

Figure 4. c-Myc is directly regulated by IP_3R-dependent MEF2C expression

(A) Immunoblot analysis of pSer473 AKT, AKT, pSer235/236 S6 in control and IP_3R-TKO splenic B cells following stimulation with anti-IgM for indicated times. Data are representative of three independent experiments.

(B) ChIP-qPCR analysis of the binding of MEF2C on *Myc* promoter in splenic B cells from control and IP_3R-TKO mice. Mean ± SEM, n = 4 independent experiments.

(C) Immunoblot analysis of MEF2C in splenic B cells from control and IP_3R-TKO mice.

(D) Quantification of expression of MEF2C in (C). Mean ± SEM, n = three to four mice per group.

(E) Immunoblot analysis of MEF2C in splenic B cells from control and IP_3R-TKO mice left untreated or treated with MG132 (50 μM) for 4 h. Data are representative of two independent experiments.

(F) Expression of *Mef2c* in splenic B cells from control and IP_3R-TKO mice analyzed by qRT-PCR. Mean ± SEM, n = three to seven mice per group.

(G) ChIP-qPCR analysis of the binding of MEF2C on *Mef2c* promoter in splenic B cells from control and IP_3R-TKO mice.

Mean ± SEM, n = 4 independent experiments. For all figures, *p < 0.05.

IP_3R-TKO B cells was because of increased protein degradation or decreased transcription. Inhibition of proteasome by MG132 could lead to an increase of MEF2C protein in both control and IP_3R-TKO B cells (Figure 4E) but was still not sufficient to reverse the decline of MEF2C protein in IP_3R-TKO B cells (Figure 4E), implying that decreased MEF2C expression were not caused by protein degradation at the loss of IP_3Rs. Conversely, we found that *Mef2c* mRNA was decreased by ~50% in IP_3R-TKO B cells compared with control cells (Figure 4F), suggesting decreased transcription of MEF2C. In addition, ChIP-qPCR analysis also revealed that MEF2C could directly bind to its own promoter, but the interaction was significantly reduced in IP_3R-TKO B cells (Figure 4G), which is consistent with a previous study reporting that MEF2C could directly regulate its own transcription (Kong et al., 2016). Taken together, our results suggest that IP_3R deficiency may have led to reduced MEF2C expression, which further impaired c-Myc and its downstream targets to disrupt metabolic reprogramming in B cells upon BCR stimulation.

DISCUSSION

B cells are exposed to changing environments and are transiently switching between quiescent stages and stages of rapid proliferation or increased protein secretion (Egawa and Bhattacharya, 2019). Consequently,

nutrient uptake and activity of the B cell metabolic pathways must also be dynamically reprogrammed to meet the adjusting metabolic demands (Jellusova, 2018). Although much attention has been focused on the function of nutrient transporters and metabolic enzymes (e.g., mTORC1) (Ben-Sahra and Manning, 2017; Jellusova and Rickert, 2016), we reasoned that intracellular Ca^{2+} elevation, being one of the earliest downstream signaling events in response to BCR ligation, may be involved in triggering B cell metabolic activation. Using the IP_3R triple knockout model in which Ca^{2+} release and subsequent SOCE were abolished (Tang et al., 2017), we demonstrated that IP_3R-Ca^{2+} and calcineurin play a critical role in metabolic reprogramming of B cells during its activation and proliferation. IP_3R-Ca^{2+}-calcineurin not only regulates glucose uptake and glycolytic enzyme expression but also induces mitochondrial remodeling in activated B cells. In addition, we identified MEF2C and c-Myc as the likely downstream targets of the IP_3R-mediated Ca^{2+} signaling in activating the BCR-induced metabolic switch. Therefore, in addition to the currently known intracellular messengers of metabolism adaptations, such as ATP and ROS, our study proposes a novel role for Ca^{2+}, the most tightly regulated but dynamic signaling molecule, as the metabolic trigger for B cell activation and proliferation, which may be important in understanding the immunodeficiency of IP_3R-related diseases.

The importance of IP_3R and Ca^{2+} signaling in immune function was demonstrated in a recent report that identified variants in IP_3R subtype 3 as the underlying cause for disturbed Ca^{2+} signaling resulting in immunodeficiency in humans (Neumann et al., 2021). A reduction of IP_3R subtype 3 expression at the mRNA and protein level was found in the patient's mononuclear cells. Though abnormal proliferation and activation responses following BCR ligation in patient cells was observed, the underlying mechanism was not interrogated. Thus, our findings that loss of IP_3R and/or inhibition of calcineurin leads to the inactivation of metabolic reprogramming of B cells, which impairs proliferation and survival in response to BCR stimulation, thus provide a likely explanation to the immunodeficiency and immune dysregulation observed in IP_3R-defective patients and identify IP_3R-Ca^{2+} mediated B cell metabolic pathway as diagnostic targets for patients with specific inborn errors of immunity. Whether activation of metabolic reprogramming through targeting the IP_3R-calcineurin-MEF2C-Myc axis may help remedy the disease, is worthy of future investigation.

Apart from this, calcineurin inhibitors are widely administered in clinical medicine as immunosuppressants to prevent graft-versus-host rejection and treat certain autoimmune diseases (Guada et al., 2016); although inhibition of gene expression dependent on NFAT has been attributed as the main mechanistic paradigm (Hodge et al., 1996; Peng et al., 2001; Ranger et al., 1998), their underlying mechanism in prohibiting B cell proliferation was only partially understood. Our finding that IP_3R-Ca^{2+} and calcineurin regulates B cell metabolic reprogramming thus reveals an alternative route by which calcineurin contributes to B cell proliferation, highlighting inhibition of the Ca^{2+} metabolic trigger and subsequent impairment of glucose uptake, glycolytic enzyme expression, and mitochondrial remodeling as the primary cause of immune-suppression. In addition, calcineurin inhibitors like CsA are associated with a number of side effects because of their high toxicity, such as carcinogenicity (Guada et al., 2016); therefore, there is substantial interest in developing targeted alternatives to CsA that maintain immunosuppressive function but with fewer off-target effects (Waldmeier et al., 2003). In this regard, targeting IP_3Rs with antagonists (such as IRBIT (Gambardella et al., 2021)) to specifically block B cell metabolic reprogramming and proliferation may prove to be a more targeted approach in treating autoimmune diseases or immune rejection.

Mechanistically, we reveal that MEF2C-dependent regulation of c-Myc may be important for IP_3R-mediated calcium signaling in regulating BCR-induced metabolic reprogramming. Interestingly, MEF2C has been reported to express at a low protein level and exhibit impaired DNA-binding activity in transitional B cells compared to naive mature B cells (Andrews et al., 2012). This is in agreement with our finding that IP_3R-deficient B cells are similar to transitional B cells, which undergo apoptosis rather than survive and proliferate upon BCR stimulation, possibly because of reduced MEF2C expression and activity. Notably, we found that MEF2C binds to the promoter region of *Myc*, suggesting that IP3R-dependent MEF2C expression modulates c-Myc induction. This is supported by previous studies that found: 1) enforced expression of MEF2C in transitional B cells enhances cell proliferation, survival, and expression of *Myc* transcripts (Andrews et al., 2012), and 2) MEF2C controls MYC expression by regulating the activity of MYC Epstein-Barr virus super-enhancers (ESEs) in lymphoblastoid cell lines (Wang et al., 2019), corroborating a direct role of MEF2C in c-Myc expression. However, it should be noted that calcineurin may also

affect other molecules and pathways that can have an impact on metabolism independently of c-Myc, such as the transcriptional factor EB (TFEB), a known substrate of calcineurin and a master regulator of lysosomal biogenesis and autophagy (Medina et al., 2015). Alternatively, Ca^{2+} has been shown to directly impact cellular energy metabolism in skeletal muscle through modulating the mitochondrial ETC and the F1F0 ATP synthase (Glancy et al., 2013).

Collectively, our study revealed IP_3R-mediated Ca^{2+} signaling as one of the earliest triggering events in B cell activation and metabolic reprogramming by coordinated regulation of glucose uptake, glycolytic enzyme expression, and mitochondrial remodeling, likely through the calcineurin-MEF2C-Myc pathway, which may provide mechanistic insights into the disease etiology of immunodeficiency patients with IP_3R mutations and the pharmacological mechanism of calcineurin inhibitors.

Limitations of the study

Although we found that IP_3R-mediated Ca^{2+} signaling is essential for B cell activation and proliferation through regulating metabolic reprogramming, our results also showed that at least in some instances (for example cell proliferation), anti-IgM in IP_3R-TKO B cells still produced somewhat of an effect, which may implicate a (minor) role for Ca^{2+}-independent effects or Ca^{2+}-dependent effects mediated through other channels besides IP_3Rs. Another limitation of this study is that we have not tested other types of BCR stimulation, such as IgD, which based on past literature may produce effects different than that of anti-IgM.

STAR★METHODS

Detailed methods are provided in the online version of this paper and include the following:

- KEY RESOURCES TABLE
- RESOURCE AVAILABILITY
  - Lead contact
  - Materials availability
  - Data and code availability
- EXPERIMENTAL MODEL AND SUBJECT DETAILS
  - Animals
  - B cell isolation and culture
- METHOD DETAILS
  - Cellular calcineurin activity assay
  - Extracellular flux analysis
  - Real-time PCR
  - Immunoblotting
  - Flow cytometry
  - Glucose uptake measurement
  - ChIP assay
- QUANTIFICATION AND STATISTICAL ANALYSIS

SUPPLEMENTAL INFORMATION

Supplemental information can be found online at https://doi.org/10.1016/j.isci.2022.104209.

ACKNOWLEDGMENTS

The authors would like to thank Ju Chen (University of California, San Diego) for critical reading of our manuscript. This work was supported by the National Science Foundation of China (81970421, 82170235 to K.O., 31800767 to H.T.), the Shenzhen Science and Technology Program (KCXFZ20201221173203009 to Y.L.), the Shenzhen Basic Research Foundation (JCYJ20190808174001746, JCYJ20210324105407019 to K.O., JCYJ20180301170636978 to Y.G., JCYJ20180507183224565 to Y.L., JCYJ20210324105603009, JCYJ20210324110012034 to L.H.), the Shenzhen-Hong Kong Institute of Brain Science-Shenzhen Fundamental Research Institutions (2019SHIBS0004 to K.O.), and the Shenzhen Science and technology innovation committee project (JCYJ20180507182239272 to C.W.).

AUTHOR CONTRIBUTIONS

H.T., Y.L., S.W., J.J., X.Z., C.H., Y.L., L.H., Y.G., and L.S. performed the experiments. H.T., J.L., and K.O. designed the research. H.T., Y.L., Y.B., X.F., L.S., C.W., and K.O. wrote the manuscript.

DECLARATION OF INTERESTS

The authors declare no competing interests.

Received: November 29, 2021
Revised: March 5, 2022
Accepted: April 4, 2022
Published: May 20, 2022

REFERENCES

Akkaya, M., Traba, J., Roesler, A.S., Miozzo, P., Akkaya, B., Theall, B.P., Sohn, H., Pena, M., Smelkinson, M., Kabat, J., et al. (2018). Second signals rescue B cells from activation-induced mitochondrial dysfunction and death. Nat. Immunol. *19*, 871–884.

Andrews, S.F., Dai, X., Ryu, B.Y., Gulick, T., Ramachandran, B., and Rawlings, D.J. (2012). Developmentally regulated expression of MEF2C limits the response to BCR engagement in transitional B cells. Eur. J. Immunol. *42*, 1327–1336.

Baba, Y., and Kurosaki, T. (2011). Impact of Ca2+ signaling on B cell function. Trends Immunol. *32*, 589–594.

Baba, Y., and Kurosaki, T. (2016). Role of calcium signaling in B cell activation and biology. Curr. Top. Microbiol. Immunol. *393*, 143–174.

Ben-Sahra, I., and Manning, B.D. (2017). mTORC1 signaling and the metabolic control of cell growth. Curr. Opin. Cell Biol. *45*, 72–82.

Berry, C.T., Liu, X., Myles, A., Nandi, S., Chen, Y.H., Hershberg, U., Brodsky, I.E., Cancro, M.P., Lengner, C.J., May, M.J., et al. (2020). BCR-induced Ca(2+) signals dynamically tune survival, metabolic reprogramming, and proliferation of naive B cells. Cell Rep. *31*, 107474.

Blaeser, F., Ho, N., Prywes, R., and Chatila, T.A. (2000). Ca(2+)-dependent gene expression mediated by MEF2 transcription factors. J. Biol. Chem. *275*, 197–209.

Caro-Maldonado, A., Wang, R., Nichols, A.G., Kuraoka, M., Milasta, S., Sun, L.D., Gavin, A.L., Abel, E.D., Kelsoe, G., Green, D.R., et al. (2014). Metabolic reprogramming is required for antibody production that is suppressed in anergic but exaggerated in chronically BAFF-exposed B cells. J. Immunol. *192*, 3626–3636.

Chen, F., Chen, J., Wang, H., Tang, H., Huang, L., Wang, S., Wang, X., Fang, X., Liu, J., Li, L., et al. (2021a). Histone lysine methyltransferase SETD2 regulates coronary vascular development in embryonic mouse hearts. Front. Cell Dev. Biol. *9*, 651655.

Chen, Z., Zhu, S., Wang, H., Wang, L., Zhang, J., Gu, Y., Tan, C., Dhanani, M., Wever, E., Wang, X., et al. (2021b). PTPMT1 is required for embryonic cardiac cardiolipin biosynthesis to regulate mitochondrial morphogenesis and heart development. Circulation *144*, 403–406.

Diaz-Munoz, M.D., Bell, S.E., Fairfax, K., Monzon-Casanova, E., Cunningham, A.F., Gonzalez-Porta, M., Andrews, S.R., Bunik, V.I., Zarnack, K., Curk, T., et al. (2015). The RNA-binding protein HuR is essential for the B cell antibody response. Nat. Immunol. *16*, 415–425.

Donnelly, R.P., and Finlay, D.K. (2015). Glucose, glycolysis and lymphocyte responses. Mol. Immunol. *68*, 513–519.

Dufort, F.J., Gumina, M.R., Ta, N.L., Tao, Y., Heyse, S.A., Scott, D.A., Richardson, A.D., Seyfried, T.N., and Chiles, T.C. (2014). Glucose-dependent de novo lipogenesis in B lymphocytes: a requirement for atp-citrate lyase in lipopolysaccharide-induced differentiation. J. Biol. Chem. *289*, 7011–7024.

Egawa, T., and Bhattacharya, D. (2019). Regulation of metabolic supply and demand during B cell activation and subsequent differentiation. Curr. Opin. Immunol. *57*, 8–14.

Foster, D.A., Yellen, P., Xu, L., and Saqcena, M. (2010). Regulation of G1 cell cycle progression: distinguishing the restriction point from a nutrient-sensing cell growth checkpoint(s). Genes Cancer *1*, 1124–1131.

Gambardella, J., Morelli, M.B., Wang, X., Castellanos, V., Mone, P., and Santulli, G. (2021). The discovery and development of IP3 receptor modulators: an update. Expert Opin. Drug Discov. *16*, 709–718.

Glancy, B., Willis, W.T., Chess, D.J., and Balaban, R.S. (2013). Effect of calcium on the oxidative phosphorylation cascade in skeletal muscle mitochondria. Biochemistry *52*, 2793–2809.

Gu, M., Zhou, X., Sohn, J.H., Zhu, L., Jie, Z., Yang, J.Y., Zheng, X., Xie, X., Yang, J., Shi, Y., et al. (2021). NF-kappaB-inducing kinase maintains T cell metabolic fitness in antitumor immunity. Nat. Immunol. *22*, 193–204.

Guada, M., Beloqui, A., Kumar, M.N.V.R., Préat, V., Dios-Viéitez, M.D.C., and Blanco-Prieto, M.J. (2016). Reformulating cyclosporine A (CsA): more than just a life cycle management strategy. J. Control Release. *225*, 269–282.

Hodge, M.R., Ranger, A.M., Charles de la Brousse, F., Hoey, T., Grusby, M.J., and Glimcher, L.H. (1996). Hyperproliferation and dysregulation of IL-4 expression in NF-ATp-deficient mice. Immunity *4*, 397–405.

Jayachandran, N., Mejia, E.M., Sheikholeslami, K., Sher, A.A., Hou, S., Hatch, G.M., and Marshall, A.J. (2018). TAPP adaptors control B cell metabolism by modulating the phosphatidylinositol 3-kinase signaling pathway: a novel regulatory circuit preventing autoimmunity. J. Immunol. *201*, 406–416.

Jellusova, J. (2018). Cross-talk between signal transduction and metabolism in B cells. Immunol. Lett. *201*, 1–13.

Jellusova, J. (2020). Metabolic control of B cell immune responses. Curr. Opin. Immunol. *63*, 21–28.

Jellusova, J., and Rickert, R.C. (2016). The PI3K pathway in B cell metabolism. Crit. Rev. Biochem. Mol. Biol. *51*, 359–378.

Jellusova, J., and Rickert, R.C. (2017). A Brake for B Cell Proliferation: appropriate responses to metabolic stress are crucial to maintain B cell viability and prevent malignant outgrowth. Bioessays *39*, 1700079. https://doi.org/10.1002/bies.201700079.

Klaus, G.G., Choi, M.S., and Holman, M. (1994). Properties of mouse CD40. Ligation of CD40 activates B cells via a Ca(++)-dependent, FK506-sensitive pathway. Eur. J. Immunol. *24*, 3229–3232.

Kong, N.R., Davis, M., Chai, L., Winoto, A., and Tjian, R. (2016). MEF2C and EBF1 Co-regulate B cell-specific transcription. PLoS Genet. *12*, e1005845.

LeBien, T.W., and Tedder, T.F. (2008). B lymphocytes: how they develop and function. Blood *112*, 1570–1580.

Li, X., Luo, G., Li, T., Sun, H., Wang, W., Eiler, E., Goldsmith, J.R., and Chen, Y.H. (2020). The c-Rel-c-Myc axis controls metabolism and proliferation of human T leukemia cells. Mol. Immunol. *125*, 115–122.

Lin, Q., Zhao, G., Fang, X., Peng, X., Tang, H., Wang, H., Jing, R., Liu, J., Lederer, W.J., Chen, J., et al. (2016). IP3 receptors regulate vascular smooth muscle contractility and hypertension. JCI Insight *1*, e89402.

Lin, Q., Zhao, L., Jing, R., Trexler, C., Wang, H., Li, Y., Tang, H., Huang, F., Zhang, F., Fang, X., et al. (2019). Inositol 1,4,5-trisphosphate receptors in endothelial cells play an essential role in

vasodilation and blood pressure regulation. J. Am. Heart Assoc. *8*, e011704.

Low, M.S.Y., Brodie, E.J., Fedele, P.L., Liao, Y., Grigoriadis, G., Strasser, A., Kallies, A., Willis, S.N., Tellier, J., Shi, W., et al. (2019). IRF4 activity is required in established plasma cells to regulate gene transcription and mitochondrial homeostasis. Cell Rep. *29*, 2634–2645.e2635.

Medina, D.L., Di Paola, S., Peluso, I., Armani, A., De Stefani, D., Venditti, R., Montefusco, S., Scotto-Rosato, A., Prezioso, C., Forrester, A., et al. (2015). Lysosomal calcium signalling regulates autophagy through calcineurin and TFEB. Nat. Cell Biol. *17*, 288–299.

Neumann, J., Van Nieuwenhove, E., Terry, L.E., Staels, F., Knebel, T.R., Welkenhuyzen, K., Baker, M.R., Gerbaux, M., Willemsen, M., Barber, J.S., et al. (2021). Disrupted Ca2+ homeostasis and immunodeficiency in patients with functional Inositol 1,4,5-trisphosphate receptor subtype 3 defects *medRxiv*, 2021.2005.2029.21257775.

Ouyang, K., Leandro Gomez-Amaro, R., Stachura, D.L., Tang, H., Peng, X., Fang, X., Traver, D., Evans, S.M., and Chen, J. (2014). Loss of IP3R-dependent Ca2+ signalling in thymocytes leads to aberrant development and acute lymphoblastic leukemia. Nat. Commun. *5*, 4814.

Peng, S.L., Gerth, A.J., Ranger, A.M., and Glimcher, L.H. (2001). NFATc1 and NFATc2 together control both T and B cell activation and differentiation. Immunity *14*, 13–20.

Ranger, A.M., Oukka, M., Rengarajan, J., and Glimcher, L.H. (1998). Inhibitory function of two NFAT family members in lymphoid homeostasis and Th2 development. Immunity *9*, 627–635.

Scarpulla, R.C. (2011). Metabolic control of mitochondrial biogenesis through the PGC-1 family regulatory network. Biochim. Biophys. Acta *1813*, 1269–1278.

Tang, H., Wang, H., Lin, Q., Fan, F., Zhang, F., Peng, X., Fang, X., Liu, J., and Ouyang, K. (2017). Loss of IP3 receptor-mediated Ca(2+) release in mouse B cells results in abnormal B cell development and function. J. Immunol. *199*, 570–580.

Vaeth, M., and Feske, S. (2018). NFAT control of immune function: New Frontiers for an Abiding Trooper. F1000Res. *7*, 260.

Vaeth, M., Maus, M., Klein-Hessling, S., Freinkman, E., Yang, J., Eckstein, M., Cameron, S., Turvey, S.E., Serfling, E., Berberich-Siebelt, F., et al. (2017). Store-operated Ca(2+) entry controls clonal expansion of T cells through metabolic reprogramming. Immunity *47*, 664–679.e6.

Waldmeier, P.C., Zimmermann, K., Qian, T., Tintelnot-Blomley, M., and Lemasters, J.J. (2003). Cyclophilin D as a drug target. Curr. Med. Chem. *10*, 1485–1506.

Wang, C., Jiang, S., Zhang, L., Li, D., Liang, J., Narita, Y., Hou, I., Zhong, Q., Gewurz, B.E., Teng, M., et al. (2019). TAF family proteins and MEF2C are essential for Epstein-Barr virus super-enhancer activity. J. Virol. *93*, e00513–19.

Wang, R., and Green, D.R. (2012). Metabolic checkpoints in activated T cells. Nat. Immunol. *13*, 907–915.

Wick, A.N., Drury, D.R., Nakada, H.I., Wolfe, J.B., Britton, B., and Grabowski, R. (1957). Localization of the primary metabolic block produced by 2-deoxyglucose. J. Biol. Chem. *224*, 963–969.

Wilker, P.R., Kohyama, M., Sandau, M.M., Albring, J.C., Nakagawa, O., Schwarz, J.J., and Murphy, K.M. (2008). Transcription factor Mef2c is required for B cell proliferation and survival after antigen receptor stimulation. Nat. Immunol. *9*, 603–612.

STAR★METHODS

KEY RESOURCES TABLE

REAGENT or RESOURCE	SOURCE	IDENTIFIER
Antibodies		
anti-rabbit IP_3R1	Our lab	Ouyang et al., 2014
anti-rabbit IP_3R2	Our lab	Ouyang et al., 2014
anti-mouse IP_3R3	BD Biosciences	Cat# 610312; RRID:AB_397704
anti-rabbit MEF2C	Abcam	Cat# ab211493; RRID:AB_2864417
anti-rabbit Akt (pan) (C67E7)	Cell Signaling Technologies	Cat# 4691; RRID:AB_915783
anti-rabbit phospho-Akt (Ser473) (D9E)	Cell Signaling Technologies	Cat# 4060; RRID:AB_2315049
anti-rabbit phospho-S6 (Ser235/236) (D57.2.2E)	Cell Signaling Technologies	Cat# 4858; RRID:AB_916156
anti-mouse β-actin (C4)	Santa cruz	Cat# sc-47778 HRP; RRID:AB_2714189
Total Oxphos Rodent WB antibody cocktail	Abcam	Cat# ab110413; RRID:AB_2629281
anti-rabbit GLUT1 [EPR3915]	Abcam	Cat# ab115730; RRID:AB_10903230
anti-rabbit GLUT3 (FITC)	Abcam	ab136180
anti-rabbit Ki-67 (D3B5)	Cell Signaling Technologies	Cat# 9129; RRID:AB_2687446
anti-rabbit TOMM20 [EPR15581-54]	Abcam	Cat# ab186735; RRID:AB_2889972
anti-mouse VDAC1 [20B12AF2] (Alexa Fluor®488)	Abcam	ab179839
anti-mouse IgM (RMM-1) (FITC)	Biolegend	Cat# 406505; RRID:AB_315055
Alexa-647 conjugated anti-rabbit IgG secondary antibody	Invitrogen	Cat# A-21245; RRID:AB_2535813
anti-rabbit c-Myc (D84C12)	Cell Signaling Technologies	Cat# 5605; RRID:AB_1903938
Chemicals, peptides, and recombinant proteins		
AffiniPure F(ab')2 Fragment Goat Anti-Mouse IgM, Mu Chain Specific	Jackson ImmunoResearch	115-006-020
CsA	Sigma Aldrich	59865-13-3
FK506	Sigma Aldrich	109581-93-3
2-Desoxy-Glucose (2-DG)	Sigma Aldrich	154-17-6
2-NBDG	ThermoFisher Scientific	N13195
Ionomycin	Sigma Aldrich	56092-82-1
Mito-Tracker Green	Beyotime	C1048
LIVE/DEAD™ Fixable Dead Cell Stain	Invitrogen	L34971
Critical commercial assays		
Calcineurin Cellular Activity Assay Kit	Eno Life Sciences	BML-AK816-001
Seahorse XF Cell Mito Stress Test Kit	Agilent Technologies	103015-100
Chromatin IP kit	Cell Signaling Technologies	9005
TransScript One-Step gDNA Removal and cDNA Synthesis SuperMix Kit	TransGen Biotech	AH311-02
Experimental models: Organisms/strains		
Mouse: IP_3R triple-floxed: $Itpr1^{f/f}Itpr2^{f/f}Itpr3^{f/f}$	Our lab	N/A
Mouse: CD19-Cre: $Cd19^{tm1(cre)Cgn}/J$	The Jackson Laboratory	006785; RRID:IMSR_JAX:006785
Oligonucleotides		
Primers for qPCR	See Table S1	N/A

(Continued on next page)

Continued

REAGENT or RESOURCE	SOURCE	IDENTIFIER
Software and algorithms		
GraphPad Prism version 8.0.0	GraphPad Software, San Diego, California USA	https://www.graphpad.com/scientific-software/prism
FACSDiva software	BD Biosciences	https://www.bdbiosciences.com/en-us/products/software/instrument-software/bd-facsdiva-software
FlowJo software	BD Biosciences	https://www.flowjo.com/

RESOURCE AVAILABILITY

Lead contact

Further information about the protocols and requests for resources and reagents should be directed to and will be fulfilled by the lead contact, Huayuan Tang (tanghuayuan33@126.com).

Materials availability

This study did not generate new unique reagents.

Data and code availability

All data reported in this paper will be shared by the lead contact upon request.

This paper does not report original code.

Any additional information required to reanalyze the data reported in this paper is available from the lead contact upon request.

EXPERIMENTAL MODEL AND SUBJECT DETAILS

Animals

IP_3R triple-floxed (*Itpr1*$^{f/f}$*Itpr2*$^{f/f}$*Itpr3*$^{f/f}$) mice have been described previously (Lin et al., 2016, 2019; Ouyang et al., 2014). *Itpr1*$^{f/f}$*Itpr2*$^{f/f}$*Itpr3*$^{f/f}$ mice were crossed with Cd19$^{tm1(cre)Cgn}$/J (CD19-Cre) mice (The Jackson Laboratory). *Itpr1*$^{f/f}$*Itpr2*$^{f/f}$*Itpr3*$^{f/f}$ *Cd19cre*$^{+}$ mice were used as B cell-specific IP_3R triple knockout (IP_3R-TKO) mice. *Itpr1*$^{f/f}$*Itpr2*$^{f/f}$*Itpr3*$^{f/f}$ *Cd19cre*$^{-}$ mice were used as control mice. All mice were on a pure C57BL/6 genetic background. Male and female mice were used between 8 and 16 weeks of age. All mice were housed under specific pathogen-free conditions with a 12/12 h day/night cycle. All animal care and use procedures in this study were approved by the Institutional Animal Care and Use Committee.

B cell isolation and culture

Single-cell suspensions were obtained from spleens of control and IP_3R-TKO mice. After RBCs were depleted by hypotonic lysis, splenic B cells were purified by the negative selection of CD43^{+} cells with anti-CD43 magnetic beads (Invitrogen, 11422D). The purity of the B cells (B220^{+}) was > 95% determined by FACS analysis. Splenic B cells were stimulated in RPMI 1640 medium (supplemented with 10% FBS, 2 mM L-glutamine, 50 μM 2-mercaptoethanol and 100 U/ml penicillin plus streptomycin) with 20 μg/ml anti-IgM F(ab)'$_2$ (Jackson ImmunoResearch, 115-006-020), 1 μM CsA (Sigma Aldrich, 59865-13-3), 1.25 μM FK506 (Sigma Aldrich, 109581-93-3), 10 mM 2-DG (Sigma Aldrich, 154-17-6), 1 μM Ionomycin (Sigma Aldrich, 56092-82-1) or left unstimulated as indicated.

METHOD DETAILS

Cellular calcineurin activity assay

The splenic B cell extracts were prepared using reagents provided in the calcineurin cellular activity assay kit (Eno Life Sciences, BML-AK816-001). The assay was performed according to manual's instructions. The absorbance values from the assay were converted into amount of released phosphate following the manual.

Extracellular flux analysis

Oxygen consumption rates (OCR) and extracellular acidification rates (ECAR) were measured using an XFe24 Extracellular Flux Analyzer (Agilent). In brief, 1×10^6 B cells per well were resuspended in Seahorse medium (Agilent) and plated in 24-well Seahorse plates (Agilent) coated with poly-L-lysine (Sigma). Cells were maintained at 37°C in a non-CO2 incubator for at least 1 h before the assay. For the mitochondrial stress test, cells were treated sequentially with 1 μM oligomycin (an inhibitor of the ATP synthase), 10 μM protonophore Carbonyl cyanide-4- (trifluoromethoxy) phenylhydrazone (FCCP) and 1 μM rotenone plus 1 μM antimycin A (inhibitors of complex I and III of the respiratory chain, respectively). The basal oxygen consumption rate (OCR) was calculated by subtracting the OCR after rotenone and antimycin A treatment from the OCR before oligomycin treatment. The maximal OCR was calculated by subtracting the OCR after rotenone and antimycin A treatment from the OCR measured after addition of FCCP.

Real-time PCR

Total RNA was extracted using TRIzol reagent (Invitrogen) or RNeasy Mini Kit (Qiagen), and cDNA was synthesized using TransScript One-Step gDNA Removal and cDNA Synthesis SuperMix Kit (TransGen Biotech) as previously described (Chen et al., 2021b). Quantitative real-time PCR (RT-PCR) was performed using TransStart Tip Green qPCR SuperMix (TransGen Biotech) according to the manufacturer's instructions. The primer sequences for *Bcl2la1*, *Bcl2l1*, *Myc*, *Rel*, *Irf4*, *Pprc1*, *Hk2*, *Aldoa*, *Pgam1*, *Pkm2*, *Ldha*, *Mef2c* and 18s rRNA are presented in Table S1. Relative transcript abundance was normalized to 18S ribosomal RNA (18S rRNA). Each sample was run at least in duplicate.

Immunoblotting

Protein analysis was performed as previously described (Chen et al., 2021a). In brief, total cell lysates were prepared in lysis buffer containing 8 M urea, 2 M thiourea, 3% SDS, 75 mM DTT, 0.05 M Tris-HCl [pH 6.8], and 0.03% bromophenol blue. Lysates from equal numbers of cells for each condition were subjected to SDS-PAGE and analyzed by Western blotting using the following antibodies: anti-IP_3R1 (Ouyang et al., 2014), anti-IP_3R2 (Ouyang et al., 2014), anti-IP_3R3 (BD Biosciences, 610312), anti-MEF2C (Abcam, ab211493), anti-c-Myc (Cell Signaling Technologies, 5605), anti-panAkt (Cell Signaling Technologies, 4691), anti-Akt p-Ser473 (Cell Signaling Technologies, 4060), anti-S6 p-Ser235/236 (Cell Signaling Technologies, 4858), anti-β-actin (Santa cruz, sc-47778), and Total Oxphos Rodent WB antibody cocktail (Abcam, ab110413). Proteins were visualized using an HPR-conjugated anti-mouse or anti-rabbit secondary antibody (Cell Signaling Technologies) and chemiluminescent ECL reagent (Thermo Fisher). Densitometric quantification was performed using ImageJ.

Flow cytometry

Cells were washed in ice-cold PBS containing 1% FBS before blocking with anti-FcgRII/FcgRIII antibodies (2.4G2, eBioscience). Staining of surface molecules with fluorescently labeled antibodies was performed at room temperature for 20 min in the dark. GLUT1 or GLUT3 expression was detected in cells fixed and permeabilized with the IC Staining Buffer Kit (BioLegend) using a polyclonal rabbit anti-GLUT1 antibody (Abcam, ab115730) together with an Alexa-647 conjugated anti-rabbit IgG secondary antibody (Invitrogen) or a polyclonal, FITC-conjugated anti-GLUT3 antibody (Abcam, ab136180). Samples were acquired on a LSRII flow cytometer using FACSDiva software (BD Biosciences) and further analyzed with FlowJo software (Tree Star).

Glucose uptake measurement

Glucose uptake was analyzed directly using the fluorescent glucose analog 2-NBDG (ThermoFisher Scientific). Stimulated and unstimulated cells were incubated in glucose-free RPMI medium containing 100 μM 2-NBDG for 2 hr at 37 °C and the amount of 2-NBDG taken up by viable B cells was assessed by flow cytometry after staining with Propidium iodide (PI).

ChIP assay

ChIP assay was performed using a Chromatin IP kit (Cell Signaling Technologies, 9005) according to the manual. Protein-DNA complex was immunoprecipitated with antibodies against MEF2C (Abcam, ab211493) and normal rabbit IgG (Cell Signaling Technologies, 2729). The purified DNA was quantified by qPCR to detect the enrichment of *Myc* promoter (promoter-1, forward: 5′-TAGACCGGCAGA GACTCCTC-3′; reverse: 5′-CCTGCGCAGTCCAGTAAAGT-3′; promoter-2, forward: 5′-AAATCCGAGAGC

CACAACCC-3′; reverse: 5′-CCTAGTCTGCGTTTTGCTGC-3′) and *Mef2c* promoter (promoter-1, forward: 5′-TGGAGAGGAATAGGCGTGGA-3′; reverse: 5′-AGTCCAGCCTGTGGTTTCTG-3′; promoter-2, forward: 5′-ATAGCCTGGCTCTCAGTCGTG-3′; reverse: 5′-TGGATTACTCAGCCCTCTGTTC-3′) by normalized to the total input control.

QUANTIFICATION AND STATISTICAL ANALYSIS

All data are represented as mean ± SEM. All data were assessed for normality using probability plots and the Shapiro-Wilk test for normality. The unpaired Student's t-test (parametric) or the Mann–Whitney test (non-parametric, Figures 1B and 1D) was used to assess the p value when comparing two groups. All data were analyzed using GraphPad Prism 8.0; A two-sided p value < 0.05 was considered statistically significant. *$p < 0.05$, **$p < 0.01$, ***$p < 0.001$. The number of biological replicates is indicated in all of the figures and the statistical methods are noted in the figure legends and Methods.